Fifth International Conference on Sustainable Construction Materials and Technologies. http://www.claisse.info/Proceedings.htm

FINITE ELEMENT ANALYSIS OF RC BEAMS SUBJECTED TO NON-UNIFORM CORROSION OF STEEL BARS

R. K. Biswas[1a], M. Iwanami[1b], N. Chijiwa[1c], and K. Uno[2]

[1]Dept. of Civil and Environmental Engineering, Tokyo Institute of Technology, 2-12-1-M1-21, Ookayama, Meguro-ku, Tokyo, 152-8552, Japan. [1a]E-mail: <rajib.k.aa@m.titech.ac.jp>

[2]Institute of Technology, Penta-Ocean Construction Co., Ltd., 1534-1, Yonkucho, Nasushiobara, Tochigi, 329-2746, Japan.

ABSTRACT

The structural behavior of RC beams subjected to non-uniform steel bar corrosion is studied here by developing a simplified numerical approach. At first, a modeling methodology for the steel bar corrosion is presented. Then, 3D nonlinear finite element analysis is carried out to assess the residual structural performance of RC beams with non-uniform steel bar corrosion. Obtained results from the numerical study were verified with the experimental work. Six reinforced concrete beams with identical dimensions and reinforcement layout were tested under static loading. Out of the six beams, five beams were subjected to a different level of corrosion using an electrochemical method, and another beam was used as a control specimen without corrosion. Results from the experimental and numerical study demonstrated that non-uniform corrosion of steel bars led to a significant decrease in the load carrying capacity and ductility of the RC beams. Findings of this study will be useful in assessing the residual structural performance of the RC structures with non-uniform steel bar corrosion.

Keywords: RC beam, non-uniform corrosion, finite element method, corrosion-induced cracking, residual structural performance

INTRODUCTION

Corrosion of reinforcing bars is considered as one of the predominant deterioration issues of reinforced concrete structures in service. The consequences of corrosion are low load carrying capacity, less ductility, deterioration in steel-concrete bond, cracking or spalling of cover concrete and so on. As a result, corrosion affected structures gradually lose its serviceability, functionality and eventually structural safety.

In concrete, reinforcing steel bars are embedded where a dense passivating film of ϒ-iron oxide is formed and provides a non-aggressive environment to reinforcing steel. However, some existing RC structures might be constructed with low strength concrete and/or had an insufficient thickness of cover concrete. Therefore, due to insufficient thickness, low strength concrete and the difference in the ambient environments, the reinforcing steel bars in RC structural members might be subjected to a different extent of non-uniform corrosion. The concentration of chloride ion can be considered as the main reason for non-uniform or pitting corrosion in the reinforcing steel (Tuutti, 1982). Many previous studies have been devoted to understand the effect of corrosion of the reinforcing steel bar on the structural performance of RC members by the experimental study (Ou et al. 2012; Ma et al. 2012; Azam et al. 2012). A number of studies also investigated the mechanical behavior of steel bar subjected to corrosion (Castel et al. 2000; Cairns et al. 2005; Zhu et al. 2013). Another group of studies investigated the effect of corrosion on the steel-concrete bond (Al-Sulaimani et al. 1990; Stanish et al. 1997; Sæther 2011). Comparatively less attention has been devoted to the assessment of the residual structural capacity of corroded RC members using finite element method, however, this has been investigated by several researchers (Coronelli et al. 2004; Kallias et al. 2010; Hanjari et al. 2012). Interestingly, none of the studies particularly deals with finite element analysis of RC beams subjected to non-uniform corrosion.

Finite element analyses can be used to provide a reliable assessment of the strength and integrity of damaged or deteriorated structure (Vecchio 2001). Therefore, it can become a useful tool to obtain appropriate maintenance method of the deteriorated structure by understanding the influence of corrosion on the structural performance.

In this study, a simplified modeling methodology for steel bar corrosion is presented that can predict the residual structural capacity of RC beams with non-uniform steel bar corrosion. Corrosion-induced damage in RC beams is modeled by considering corrosion-induced cracking, changing the property of concrete and steel, and modifying the bond between steel and concrete.

3D NONLINEAR FINITE ELEMENT MODEL OF CORRODED RC BEAM

General

Corrosion process initiates when the dense passive film upon the reinforcing steel becomes thermodynamically unstable or broken. The passive film can be broken due to the concentration of chloride ions. After the initiation of corrosion in the reinforcing steel, the corrosion product starts growing in volume. The volumetric expansion of corrosion product can exceed 2-6 times to the original steel, and that exerts pressure on the surrounding concrete. That pressure causes tensile stresses in the surrounding concrete and ultimately leads to cracking in the concrete (Liu et al. 1998) as shown in **Figure 1.**

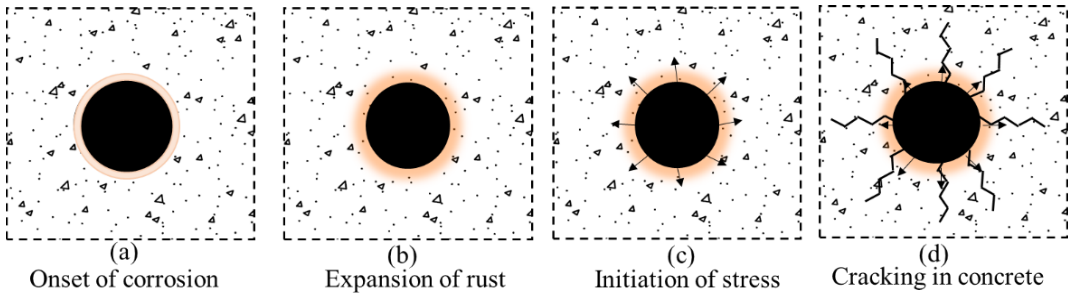

Figure 1. Corrosion process in concrete

Modeling of Concrete

Mechanical properties of concrete at a different distance from reinforcement is significantly different. In this model, the concrete domain is modeled into two categories namely plain zone (PL) and RC zone as described in An et al. (1997) and Maekawa et al. (2003). Concrete, which is confined by a reinforcing steel bar, will exhibit stable stress release due to the effect of the bond between steel and concrete.

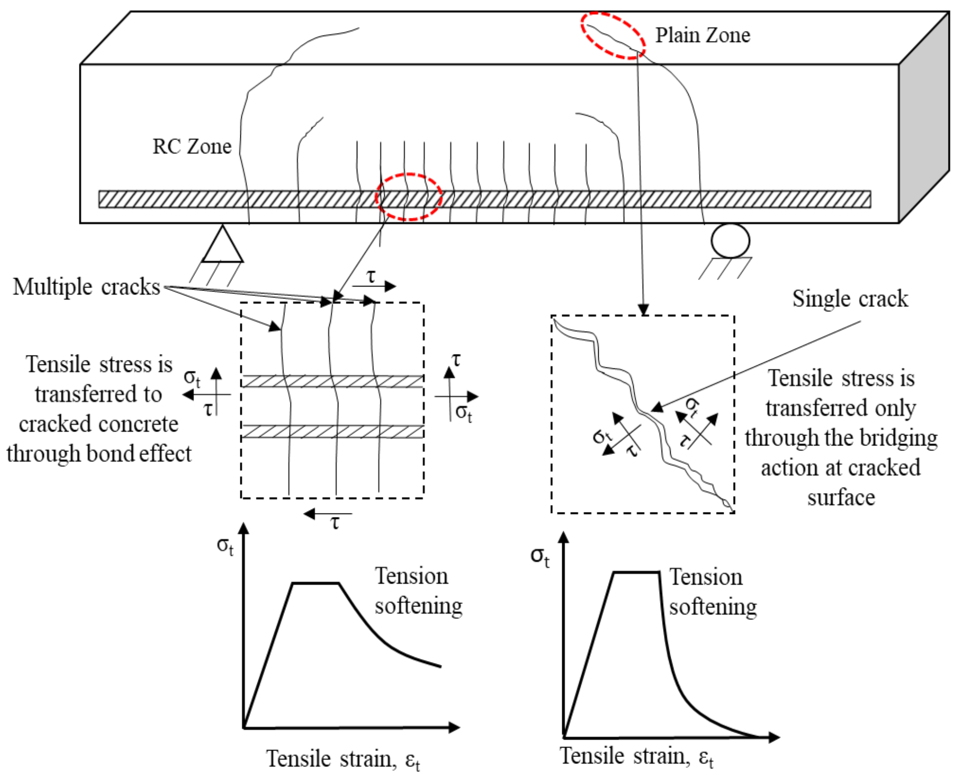

Figure 2. Concept of RC and plain zone in concrete

Whereas, the concrete outside the bond effective zone will behave as like plain concrete with sharp strain softening characteristics. This happens because the tensile stress is transferred only through bridging action at the crack surface. **Figure 2** represents the zoning concepts of RC and plain zone. It should be noted that tension-softening of plain concrete also depends on the length of the finite element. Details can be found in Maekawa et al. (2003).

Modeling of Corrosion-Induced Cracking

To simulate deteriorated RC structures effectively, mechanical damages caused by corrosion crack should be taken into account (Yoon et al. 2000; Coronelli et al. 2004). In this study, Toongoenthong-Maekawa model (Toongoenthong et al. 2005; Toongoenthong et al. 2005) is utilized to model corrosive substance and corrosion induced cracking. Here, corrosion product with non-corroded steel and surrounding concrete are assumed as a two-phase problem. The volume of expansive corrosion product can be calculated as

$$V_{corr} = \frac{\gamma \alpha \pi D^2}{4} \tag{1}$$

Where α is considered as expansion coefficient of corroded substance, ϒ represents the volume fraction loss of steel per unit length ranging from 0 to 1 (0 means no loss in the reinforcement section, and 1 means complete loss of reinforcement section), D denotes the steel diameter (m).

The reinforcement free-expansion strain of isotropy can be calculated as

$$\varepsilon_{s,free} = \sqrt{1+\gamma(\alpha-1)} - 1 \tag{2}$$

The stress induced by resistant of the surrounding concrete can be computed by multiplying the total strain of the corroded system with its average stiffness. The average stiffness of the corroded system can be expressed as

$$E_{s,eq} = \frac{1+\gamma(\alpha-1)}{(1-\frac{\gamma}{E_s}) + (\gamma\alpha / \mathrm{G})} \tag{3}$$

Where G is the stiffness of the corroded substance (~7 GPa), and E_s is the stiffness of steel (~200 GPa). In this model, a linear relationship is considered between corrosive substance and induced stress inside the concrete as shown in **Figure 3 (b)**. However, when corrosion product reaches the critical amount, the corrosion cracks progress to the concrete surface (Oh et al. 2009). After that, the corrosion products are discharged to the outside of the concrete as shown in **Figure 3 (a).** Therefore, in this proposed model, it is considered that tensile stress in concrete due to the expansion of the corrosion product becomes constant when the cracks reach the concrete surface. **Figure 3 (b)** also illustrates the proposed corrosion model, where the vertical axis represents the corrosion induced tensile stress in concrete, and the horizontal axis represents the amount of mass loss of the steel bar. The crack generation limit can be calculated by the following equation:

Crack generation limit= Cross-sectional area of rebar * critical corrosion amount* unit weight of rebar (4)

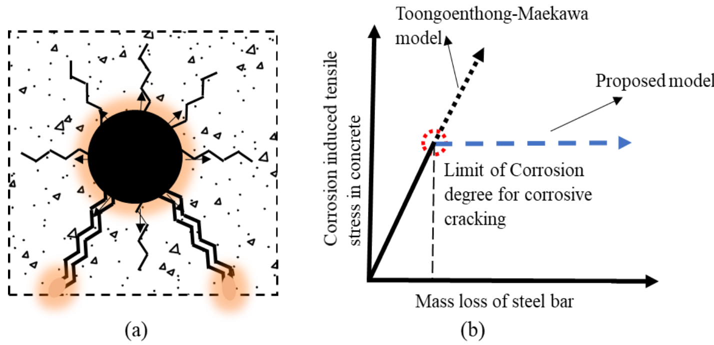

Figure 3. Corrosion induced stress in concrete

Critical corrosion amount can be calculated by the following equation (Oh et al. 2009):

$$W_{cr} = 0.0018c^{2.07} \tag{5}$$

Where W_{cr} is the critical amount of corrosion and c is the cover thickness.

Modeling of Corroded Reinforcement

Due to the corrosion process, the effective reinforcement area will be reduced. In this model, the loss of corroded steel is represented by reduced reinforcement ratio. When experimental results are available, the cross-sectional area of the corroded reinforcing steel bar can be calculated by the following equations:

$$A_S(X_{CR}) = \frac{\pi D^2}{4}\left(1 - \frac{X_{CR}}{100}\right) \tag{6}$$

$$X_{CR} = \frac{W_0 - W_C}{W_0} * 100 \tag{7}$$

Where W_o and W_c is the weight of the sound and corroded reinforcements, X_{cr} represents the corrosion ratio. When the experimental results are unavailable, corrosion amount can be predicted from the following equations (Choe et al. 2009):

$$X_{CR} = \frac{{D_{b0}}^2 - {D_b}^2}{{D_{b0}}^2} * 100 \tag{8}$$

$$D_b = D_{b0} - \frac{1.05081\left(1 - \frac{w}{c}\right)^{-1.64}}{d_C} * (\mathrm{t} - T_{cr})^{0.71} \tag{9}$$

Where D_b and D_{b0} are the diameters for the corroded and un-corroded reinforcing bars, T_{cr} is the initiation time of corrosion and t is the time after corrosion starts, d_c is the cover depth, and w/c represents the variable water-cement ratio.

Modeling of Bond Deterioration

In this study, bond deterioration between steel and concrete is modeled implicitly. Macroscopic bond deterioration is considered through considering section penetrating corrosion-induced cracking, and microscopic bond deterioration is considered around steel reinforcement by degradation in tension softening parameter (Maekawa et al.

2003).

EXPERIMENTAL STUDY AND VALIDATION OF THE PROPOSED MODEL

Details of the Experimental Study

In order to validate the proposed model, six RC beams with a different configuration of corrosion were tested under static loading. All RC beams had identical dimensions and reinforcement layout. The beam had a cross section of 200 x 350 mm; the cover depth was 35 mm at the bottom, and the beam length was 2000 mm as shown in **Figure 4.** Three different reinforcing steel bars: D13, D10, and D6 were used in this experiment, and the yield strengths were 463 MPa, 377 MPa, and 352 MPa respectively. The 28-day compressive strength of the concrete was 31 MPa. All beams were designed to fail in flexure. Accelerated corrosion was employed to obtain a non-uniform distribution of steel bar corrosion. Corrosion was controlled to occur in the

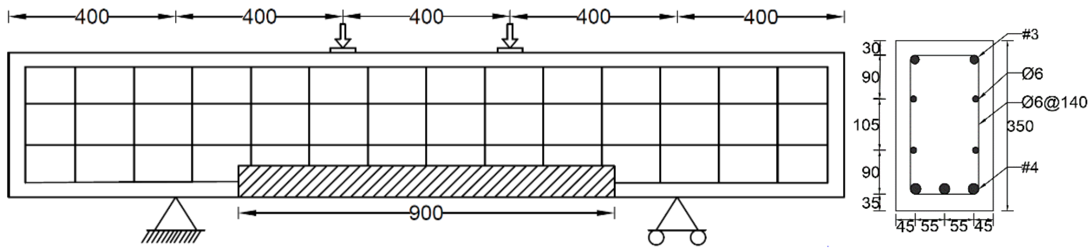

Figure 4. Details of the specimen

mid-900 mm region of the RC beams and only in tension reinforcement. After the loading test, corroded reinforcement bars were taken out from the RC beams, and average mass loss was calculated. Six different configurations of average corrosion were obtained as Case 01-sound, Case 02-17%, Case 03-26%, Case 04-11%, Case 05-17%, and Case 06-28%. Tension reinforcements were cut into small pieces (10 cm length) to know the precise distribution of the corrosion. The non-uniformity in the steel bar corrosion was found in a wide range of distribution. For example, in Case 04 (average corrosion ratio of 11%), the minimum and maximum corrosion ratio were limited to 5% and 19% respectively. Whereas, in Case 06 (average corrosion ratio of 28%), the minimum and maximum corrosion ratio were extended in the range of 11% to 60% respectively. This happened due to the difference in the accelerated corrosion test method and duration of the imposed current. Figure 5 depicts the distribution of non-uniform corrosion in the mid-900 mm of all corroded beams.

It should be noted that number of highly localized corrosion such as pit corrosion was calculated by visual observation. In this study, when the remaining diameter of the corroded bar is less than or equal to 80% of the original steel bar diameter and when the length of such a section loss along the beam axis is less than or equal to 2 cm, it is considered as highly localized corrosion. The number of highly localized corrosion was

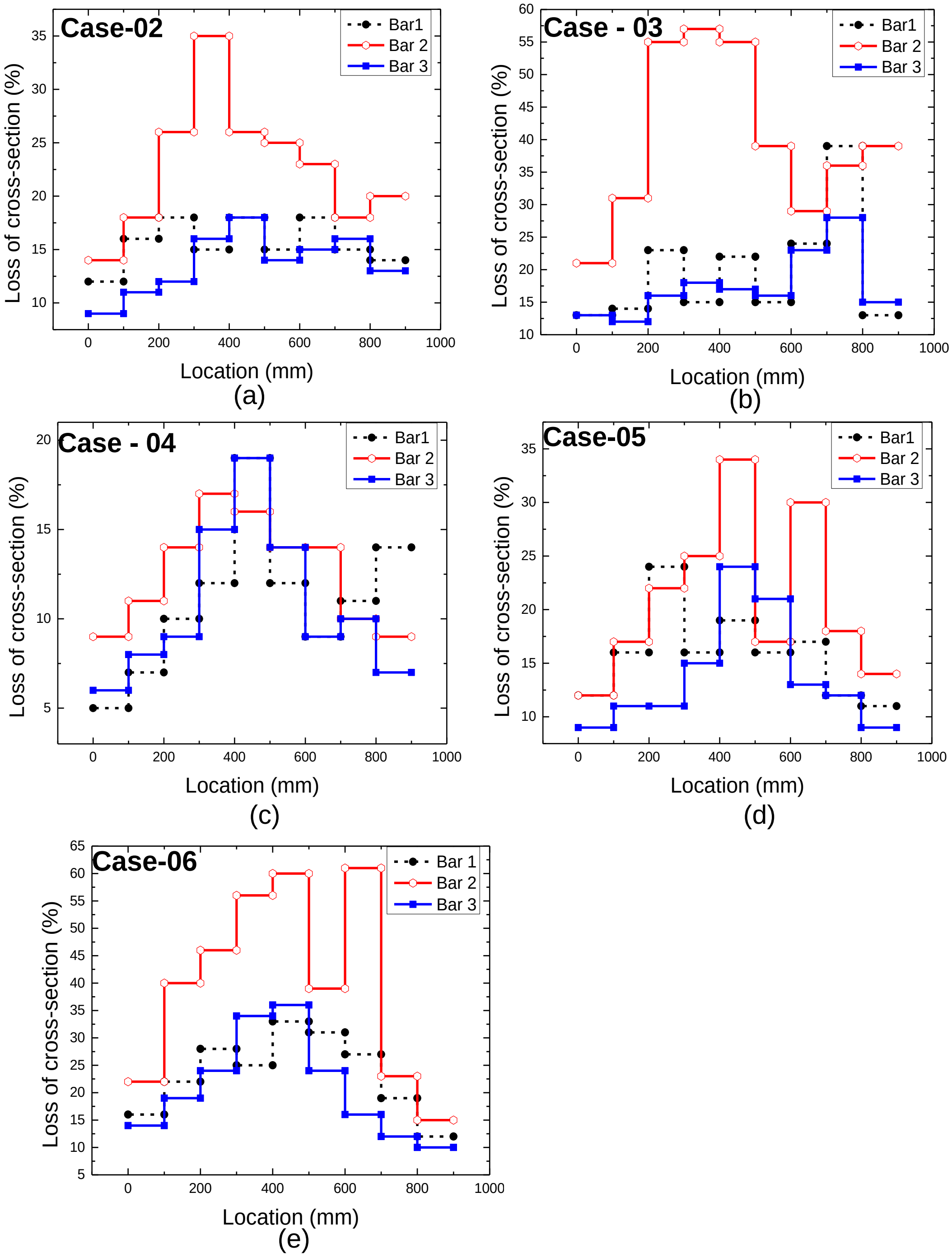

Figure 5. Distribution of corrosion for a) Case 02 b) Case 03 c) Case 04 d) Case 05 e) Case 06

10, 8, 8 and 6 for Case 02, Case 05, Case 03 and Case 06 respectively.

Validation of the Proposed Model

In this study, FEM software COM 3D was used to validate the proposed model. COM 3D is an analysis system that can reproduce the structural behavior of reinforced concrete structures considering cracking of concrete, generated stress and deformation of the member by using a nonlinear finite element method. The validity and reliability of the software can be found in the literature (Maekawa et al. 2003; Chijiwa et al. 2011; Chijiwa et al. 2015; Uno et al. 2017).

In corroded RC beams, a crack occurs due to the expansion of corrosive substance. To consider pre-existing corrosion cracks, numerical cracking was considered in the RC beam as a first step, after displacement-controlled loading was conducted. Corrosive cracking and tension softening represented bond deterioration between steel and concrete. After the experimental study, mass loss of reinforcing bars was measured for every 10 cm, and that was directly inputted into the model. Load-displacement curves

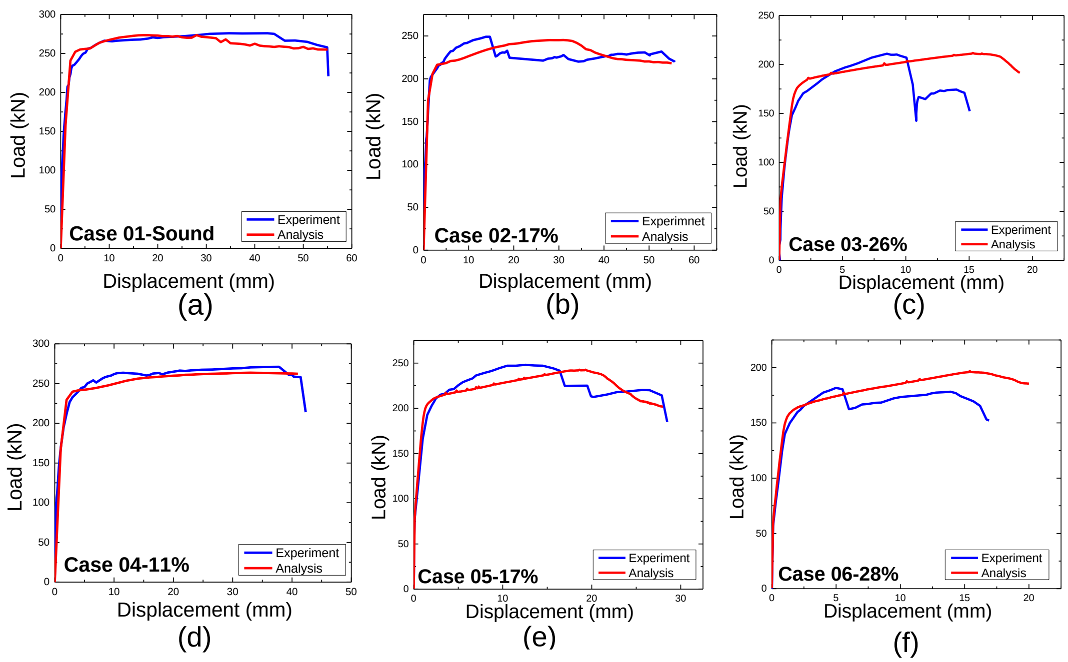

Figure 6. Comparison of load-displacement curves for a) Case 01 b) Case 02 c) Case 03 d) Case 04 e) Case 05 f) Case06

obtained from the proposed FE model had a good agreement with the experimental load-displacement curves in terms of yield and ultimate loads as shown in **Figure 6 (a-f).** Yield and ultimate loads are defined as yielding of the tension steel and ultimate capacity of the RC beams. In Case 04 (average corrosion ratio 11%), the ultimate load was computed as 262 kN, which favorably confirms the experimental value as 263 kN. Likewise, the difference between the ultimate load was 0.33%, 0.81%, 2.38%, 2.79% and 6.99% for Case 01, Case 02, Case 03, Case 05, and Case 06. The difference between yield load was 2.2%, 2.6%, 3.2%, 4.06%, 4.34% and 6.25% for Case 04, Case 02, Case 06, Case 05, Case 01 and Case03 respectively.

In order to further clarify the accuracy of the model, the cracking pattern of the corroded and non-corroded beams was compared with the experimental results. In the finite element software, COM 3D, cracks are represented by the smeared cracking model approach. Therefore, a probabilistic cracking zone can be obtained. **Figure 7** represents the comparison of crack pattern with strain distribution (0-5000μ) for different cases at the collapse of the RC beams. In the experiments, the number of cracks and cracking zone reduced significantly as the corrosion ratio increased. The proposed model captured this phenomenon with high precision.

The previously mentioned verifications of the finite element analysis indicate that the proposed model can predict the structural behavior of RC beam with non-uniform steel bar corrosion with high accuracy.

PERFORMANCE OF THE CORRODED RC BEAMS UNDER CYCLIC LOADING

The proposed numerical model was able to simulate the behavior of RC beams with non-uniform steel bar corrosion with high precision under static loading. Therefore, the effect of non-uniform corrosion on the structural performance of RC beams under cyclic loading is also investigated with the proposed model. The material properties used in the cyclic loading are the same as used in the static loading. It should be noted

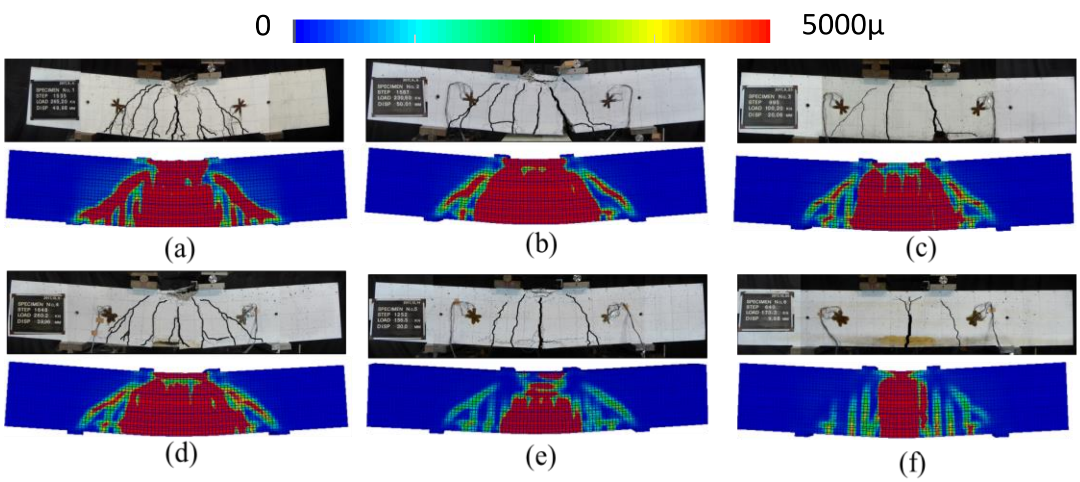

Figure 7. Comparison of crack pattern with strain distribution for a) Case 01 b) Case 02 c) Case 03 d) Case 04 e) Case 05 f) Case06

that, in the cyclic loading, compression reinforcements were considered with the same degree of non-uniform corrosion distribution as obtained in tension reinforcement. The beams were cyclically loaded for the drift levels of 0.25, 0.5, 0.75, 1.0, 1.5, 2.0, 2.5 and 3%. Drift level is defined as the displacement of the beam in mid-span divided by the effective length of the beam. **Figure 8** represents the envelop response of load-deflection hysteretic loops for each beam. A substantial decrease in the yield and the ultimate load was observed as the corrosion ratio increased. For example, yield load was reduced by 15.78%, 17.81%, 21.86% 43.92%, and 53.22% for Case 04 (11% corrosion), Case 02(17% corrosion), Case 05(17% corrosion), Case 03(26% corrosion) and Case 06(28% corrosion) respectively. However, interestingly, there was a little increase in ductility as the corrosion ratio increased up to 17%. This happened because the failure mode for the sound case was the combination of flexure and shear, whereas, in corroded cases, the failure mode was governed by flexure as shown in **Figure 9**. Due to existing cracks in corroded cases, the potential cracking zone was limited to the middle of the beam. In contrast, the potential cracking zone was propagated from the supports as well as the middle of the beam in sound case. In **Figure 9,** the strain distribution of Case 01(sound) and Case 06(28% corrosion) is presented for 1.5% drift.

CONCLUSIONS

In this study, the influence of non-uniform steel bar corrosion was investigated using 3D nonlinear finite element analysis. Based on the results of this study, the important conclusions are summarized as follows:

1. A simplified modeling methodology for steel bar corrosion was proposed considering corrosion-induced cracking, changing the property of steel and concrete and modifying the bond behavior between steel and concrete.

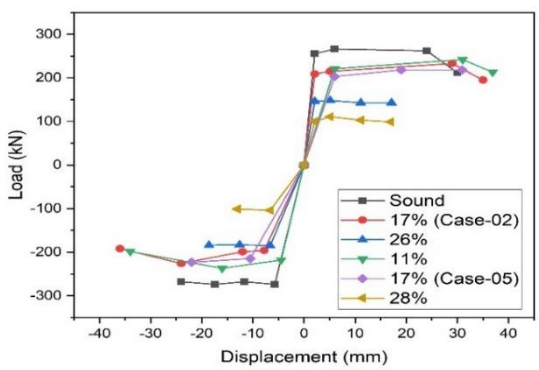

Figure 8. Envelop curves for mid-span deflection under cyclic loading

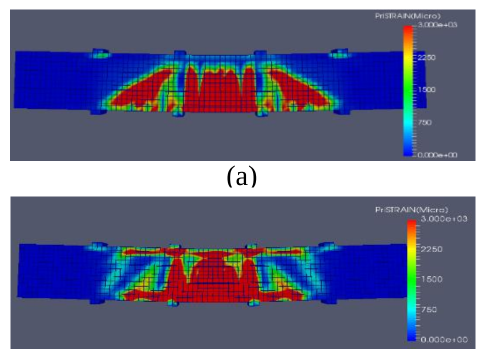

(a)

(b)

Figure 9. Strain distribution for (a) Case 01; (b) Case 06

2. The proposed model could predict the structural behavior of non-uniformly corroded RC beams with high precision in terms of yield load, ultimate load and crack patterns.
3. Non-uniform corrosion adversely affected the load carrying capacity and ductility of the RC beams.
4. The cyclic analysis revealed that ductility of the RC beams could be increased when the corrosion ratio is up to 17%.

REFERENCES

Al-Sulaimani, G. J., Kalemmullah, M., Basumbul, I. A., and Rasheeduz-zafar. (1990). "Influence of Corrosion and Cracking on Bond Behavior and Strength of Reinforced Concrete Members." *ACI Structural Journal* 87 (2), 220–231.

An, X., Maekawa, K., and Okamura, H. (1997). "Numerical Simulation of Size Effect in Shear Strength of RC Beams." *Journal of Materials, Concrete Structures and Pavement., JSCE,* 35, 297–316. doi:10.2208/jscej.1997.

Azam, R., and Soudki, K. (2012). "Structural Performance of Shear-Critical RC Deep Beams with Corroded Longitudinal Steel Reinforcement. " *Cement and Concrete Composites* 34 (8), 946–957. doi:10.1016/j.cemconcomp.2012.05.003.

Cairns, J., Plizzari, GA., Du, Y., Law, DW., and Franzoni, C. (2005). "Mechanical Properties of Corrosion-Damaged Reinforcement." *ACI Materials Journal* 102 (4), 256–264. doi:0-8493-2021-6.

Castel, A., François, R., and Arliguie, G. (2000). "Mechanical Behaviour of Corroded Reinforced Concrete Beams—Part 1: Experimental Study of Corroded Beams." *Materials and Structures* 33 (9), 539–544. doi:10.1007/BF02480533.

Chijiwa, N., Kawanaka, I., and Maekawa, K. (2011). "Effect of Strengthening at Expected Damage Zone of a RC Member with Damaged Anchorage." *Journal of Japan Society of Civil Engineers, Ser. E2 (Materials and Concrete Structures),* 67(2), 160-165 (In Japanese).

Chijiwa, N., and Maekawa, K. (2015). "Thermo-Hygral Case-Study on Full Scale RC Building under Corrosive Environment and Seismic Actions." *Journal of Advanced Concrete Technology.*, JCI, 13(10), 465-478.

Choe, D. E., Gardoni, P., Rosowsky, D., and Haukaas, T. (2009). "Seismic Fragility Estimates for Reinforced Concrete Bridges Subject to Corrosion." *Structural Safety* 31 (4), 275–283.

Coronelli, D., and Gambarova, P. (2004). "Structural Assessment of Corroded Reinforced Concrete Beams: Modeling Guidelines." *Journal of Structural Engineering.,*ASCE 130 (8), 1214–1224. doi:10.1061/(ASCE)0733-9445(2004)130:8(1214).

Hanjari, K. Z., Kettil, P., and Lundgren, K. (2012). "Analysis of Mechanical Behavior of Corroded Reinforced Concrete Structures." A*CI Materials Journal* 108 (5), 532–541.

Kallias, A. N., and Rafiq, M. I. (2010). "Finite Element Investigation of the Structural Response of Corroded RC Beams." *Engineering Structures* 32 (9), 2984–2994. doi:10.1016/j.engstruct.2010.05.017.

Liu, Y., and Weyers, R. E. (1998). "Modeling the Time-to-Corrosion Cracking in Chloride Contaminated Reinforced Concrete Structures." *ACI Materials Journal* 95 (6), 675–681. doi:10.1016/S0008-8846(98)00259-2.

Ma, Y., Che, Y., and Gong, J. (2012). "Behavior of Corrosion Damaged Circular Reinforced Concrete Columns under Cyclic Loading. " *Construction and Building Materials* 29, 548–556. doi:10.1016/j.conbuildmat.2011.11.002.

Maekawa, K., Pimanmas, A., and Okamura, H. (2003). "*Nonlinear Mechanics of Reinforced Concrete*. " Spon Press, London.

Oh, B. H., Kim, K. H., and Jang, B. S. (2009). "Critical Corrosion Amount to Cause Cracking of Reinforced Concrete Structures. " *ACI Materials Journal* 106 (4), 333–339. doi:10.14359/56653.

Ou, Y., Tsai, L., Chen, H. (2012). "Cyclic Performance of Large-scale Corroded Reinforced Concrete Beams. " *Earthquake Engineering and Structural Dynamics* 41, 593–604.

Sæther, I. (2011). "Bond deterioration of corroded steel bars in concrete." *Structure*

Infrastructure Engineering 7(6), 415–29.
Stanish, K., Hooton, R. D., and Pantazopoulou, J. (1997). "Corrosion Effects on Bond Strength in Reinforcement in Concrete. " A*CI Materials Journal* 96 (6), 915-921.
Toongoenthong, K., and Maekawa, K. (2005). "Multi-Mechanical Approach to Structural Performance Assessment of Corroded RC Members in Shear." *Journal of Advanced Concrete Technology* 3 (1), 107–122. doi:10.3151/jact.3.107.
Toongoenthong, K. and Maekawa, K. (2005). "Simulation of coupled corrosive product formation, migration into crack and propagation in reinforced concrete sections." *Journal of Advanced Concrete Technology* 3(2), 253-265
Tuutti, K. (1982). "Corrosion of Steel in Concrete." *Swedish Cement and Concrete Research Institute,* Stockholm, Sweden.
Uno, K., Chijiwa, N., Iwanami, M., Miyoshi, T., and Ogasawara, T. (2017). "Evaluation of Residual Structural Performance of Steel Pipe Piled Pier with Local Steel Bar Corrosion." *Ocean Engineering* 73 (2), 408-413.
Vecchio, F., Collins, M. P. (2001). "Nonlinear Finite Element Analysis of Reinforced Concrete: At the Crossroads? " *Structural Concrete* 2 (4), 201–212.
Yoon, S., Wang, K., Weiss, W. J., and Shah, S. P. (2000). "Interaction between Loading, Corrosion, and Serviceability of Reinforced Concrete." *ACI Structural Journal* 97 (6), 637–644. doi:10.14359/9977.
Zhu, W., Francois, R., Coroneli, D., and Cleland, D. (2013). "Effect of Corrosion of Reinforcement on the Mechanical Behaviour of Highly Corroded RC Beams." *Engineering Structures* 56, 544–554. doi:10.1016/j.engstruct.2013.04.017.